

# Blinker/Macro-spicule activity in an off-limb polar region

E. O'Shea<sup>1</sup>, D. Banerjee<sup>2</sup>, and J.G.Doyle<sup>1</sup>

<sup>1</sup> Armagh Observatory, College Hill, Armagh BT61 9DG, N.Ireland  
e-mail: eos@arm.ac.uk, e-mail: jgd@arm.ac.uk

<sup>2</sup> Indian Institute of Astrophysics, II Block, Koramangala, Bangalore 560 034, India  
e-mail: dipu@iiap.res.in

**Abstract.** Using measurements of O v 629.73Å from the Coronal Diagnostic Spectrometer (CDS) on board SOHO we report on blinker activity in off-limb regions above the Northern pole of the Sun. The blinkers are found to be occurring above a region showing strong dynamic activity, with evidence for evacuation of plasma. The presence of blinkers is discussed in terms of the heating of spicular material.

**Key words.** Sun: UV radiation – Sun: transition region – Sun: atmosphere

## 1. Introduction

The term blinker was introduced by Harrison (1997) to describe the sudden enhancement in flux observed in transition region lines with CDS. These features are found to occur preferentially on network boundaries (Harrison et al. 1999, Bewsher et al. 2002) but also in the internetwork (Brković et al. 2001), and to occur preferentially above regions of strong unipolar magnetic field (Bewsher et al. 2002). A number of papers, e.g., Madjarska & Doyle (2003), Brković & Peter (2004), Bewsher et al. (2005), have discussed blinkers and their relationship, if any, to explosive events. All conclude that explosive events and blinkers appear to be independent phenomena. Madjarska & Doyle (2003) further suggested that blinkers may just be the on-disk signatures of spicules. Also, Priest et al. (2002) discussed five different physical mechanisms for blinker formation, amongst them a heating of cool spicular material. Here, we discuss off-limb data which suggests a close relationship between blinkers and macro-spicules.

## 2. Observations and data reduction

For these observations we have used the normal incidence spectrometer (NIS), which is one of the components of the Coronal Diagnostic Spectrometer (CDS) on board the Solar and Heliospheric Observatory (SOHO), see Harrison et al. (1995). The temporal series SER150W sequence was run in December 2002 in the North polar region, during a period when the coronal hole at the poles were ill-defined. Data was obtained for 11 transition region and coronal lines. However, here we shall only discuss four of these; the transition region line of O v 629.73 Å ( $\approx 2.5 \times 10^5$  K) and the coronal lines of Mg x 609.79, 624.94 Å

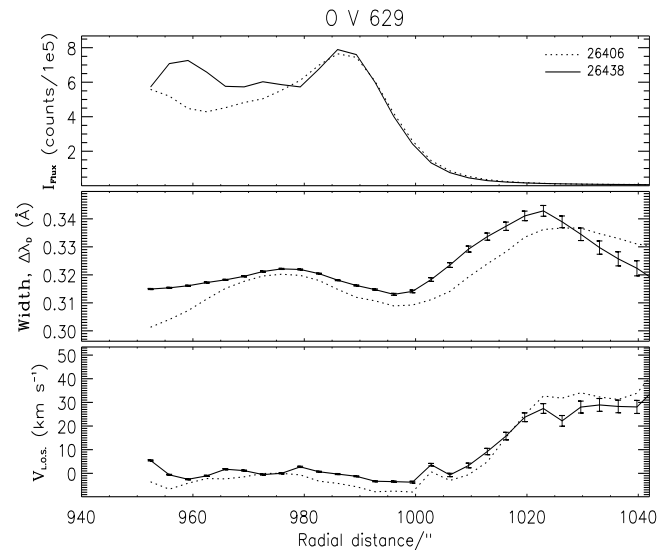


**Fig. 1.** Variation of the O v 629 flux, line width and L.O.S. velocity (top to bottom, respectively) for the 26406 and 26438 datasets.

( $\approx 1.25 \times 10^6$  K) and Si xii 520.67 Å ( $\approx 2.5 \times 10^6$  K). Note that we shall henceforth refer to the lines without the following decimal places, e.g., 629 in place of 629.73. The data was reduced using the latest versions of the standard CDS routines (see <http://solg2.bnsc.rl.ac.uk/software/uguide/uguide.shtml>). Before fitting the lines with a single Gaussian, and in order to increase the signal-to-noise ratio, we binned by 2 along the 143 pixel slit to produce 70 pixels ( $4'' \times 3.36''$ ) in Y. The line-of-sight (L.O.S.) velocities shown in this paper have all been corrected using the limb method, whereby the value of the summed profile at the limb is assumed to have an average L.O.S. velocity of zero. Scattered light was not found to make

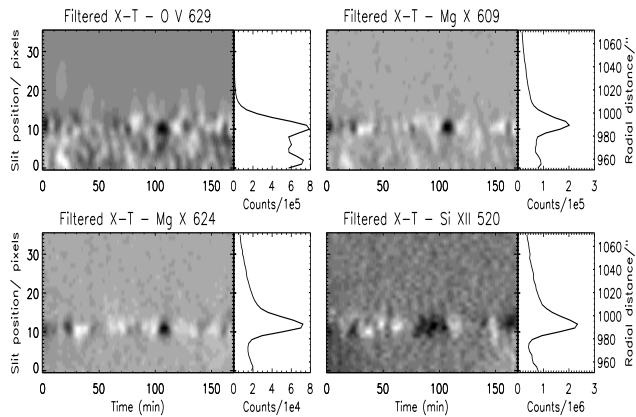


**Fig. 2.** Space-Time (X-T) plots of the radiant flux for the 26438 dataset. At the right of the plots are shown the summed fluxes over time for each pixel/radial distance along the slit.

a significant contribution to the measured flux, being present at no more than the 10% level in each of the lines, see O'Shea et al. (2005).

### 3. Results

In Fig. 1 we plot the summed over time results for the O v line showing the variation of radiant flux, line width and L.O.S. velocity as a function of slit position for the 26406 and 26438 datasets. To produce this plot we summed together 150 time frames at each pixel position along the slit and fitted the resulting summed spectral line profile. From the plot of the flux in the top panel it is apparent that both datasets show a maximum in the flux at a radial distance of  $\approx 985''$ , somewhat above the continuum limb which in these plots is located at  $\approx 975''$ . From the plots of line widths in the middle panel it can be seen that the location of the limb corresponds to an expected small increase in the line widths, due to the increased depth along the line-of-sight at this location. At the location of the maximum in the flux,  $\approx 985''$ , the line widths show a local minimum before then increasing to their maximum values at larger radial distances of between  $\approx 1000''$ – $1040''$ , coinciding with an increase in red-shifted velocities over the same range. The same behaviour is seen in both datasets. We do not plot values above  $\approx 1040''$  due to the low S/N of the O v line above this point. It is clear from Fig. 1 that there must be some dynamic activity occurring off-limb between the heights of  $\approx 1000''$ – $1040''$  to account for the large increase in the line widths. We suggest that the results seen in the O v line may be evidence for macrospicules present above the limb. The L.O.S. velocity values of  $\approx 30 \text{ km s}^{-1}$  found at the point where the O v line shows maximum line width ( $\approx 1025''$ ) in each of the datasets are consistent with those expected within macrospicules (Wilhelm 2000; Xia et al. 2005; Doyle et al. 2005).

Note, however, that we do not see strong blue-shifts above the limb, perhaps due to the averaged summed nature of this data, or the fact that, statistically, red-shifted velocities are more common off-limb. The large line widths seen in this O v line above the limb, between  $1000''$  and  $1040''$ , could be explained as being caused by high velocity events produced in the

spicule formation, i.e., as a result of magnetic reconnection. We note that Wilhelm (2000) provides evidence of a L.O.S. velocity of  $150 \text{ km s}^{-1}$  at a height of  $\sim 35$  arcsec above the limb in a macro-spicule, i.e. at approximately the same height we see the large width increases in the O v line. In order to examine these dynamic processes off-limb we plot in Fig. 2 a space-time or X-T plot, i.e., the variation of the flux with time and as a function of position along the slit for the three coronal lines and the transition region line of O v. This X-T plot has been filtered with a low-pass filter at 2 mHz, that is, periods shorter than 500s have been removed. Between  $\approx 980$ – $1000''$ , the location of the maximum flux in Fig. 1 there is clear evidence for significant dynamic activity, with the peaks and troughs of quasi-periodic oscillations apparent as white and black patches, respectively. The influence of this dynamic activity can be seen to be present up to the temperature of the Si xii line. In order to examine this activity in more detail we plot in Fig. 3 the time series plot for each of the lines at a single height of  $\approx 983''$ , i.e., pixel position no.9. From this plot the quasi-periodic nature of the activity at this location is apparent as is a significant decrease in the flux at a time of  $\approx 110$  min in the two Mg x lines and the O v line. This large decrease is apparent as the black dot at this time in the X-T plot in Fig. 2. The Si xii line shows less evidence for this large decrease at  $\approx 110$  min but the X-T plot in Fig. 2 suggests there is a decrease in flux around this time, between  $\approx 70$ – $110$  min.

We suggest that these decreases in flux are evidence of a localized evacuation of plasma. We note that the L.O.S. velocity results for each line, except Si xii, show a change from being more red-shifted to being more blue-shifted with time, suggesting a change in the direction of flow of the plasma. For the O v line the large decrease in flux at  $\approx 110$  min can be seen to be accompanied by a blue-shifted velocity at the same time. The size of the velocity shift, however, is at the margins of what can be considered statistically real as velocity measurements less than  $10$ – $15 \text{ km s}^{-1}$  are not considered reliable due to the relatively poor spectral resolution of CDS/NIS. Similarly, the possible blue-shifts in the Mg x 609 and 624 lines, which are considered unreliable due to the significant uncertainties attached to the velocity measurements. However, we can conclude that the trend of the velocity can be considered blue-shift-like. The combination of evidence for evacuated and blue-shifted plasma leads us to conclude that we are seeing a dynamic event occurring at this location. From Fig. 2 it would appear, at first glance, that there is little activity present above  $\approx 1000''$ , where we have seen the large width and velocity increases in Fig. 1. However, this is not the case as the activity is merely masked by the larger radiances closer to the limb. In order to show this, we plot, in Fig. 4 for the O v line, the X-T plot up to  $\approx 1000''$  and also from  $\approx 1000''$  up to  $\approx 1040''$ . The values in the upper panel are the square-root values of the flux. In the upper panel, the presence of weaker activity can now be seen more clearly, up to and above  $\approx 1020''$ , where the peak in the widths was seen in Fig. 1. The nature of these brightenings occurring quasi-periodically above  $1000''$  are unclear. It is possible, however, remembering the discussion of Fig. 1, to suggest that they are the signatures of macrospicules rising up to  $\approx 45''$  off-limb. In defense of this proposition, we note that none of the coronal lines shows evidence for

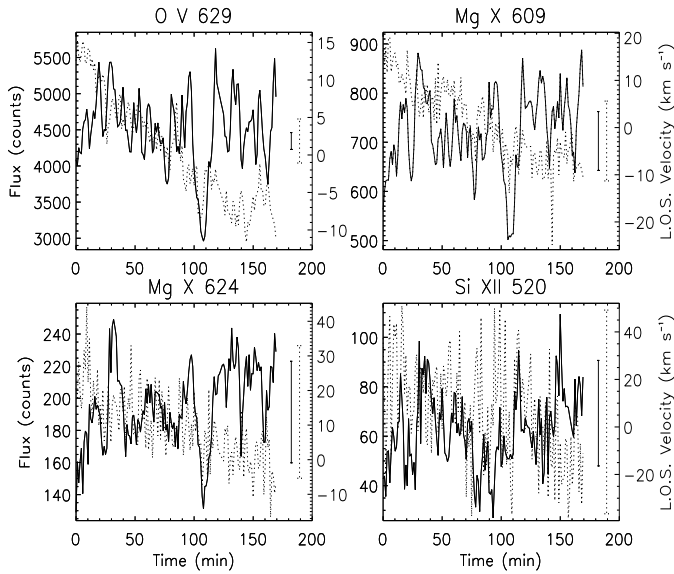


**Fig. 3.** Flux (black line) and L.O.S. velocity at a radial distance of  $\approx 983''$  in the 26438 dataset. Average uncertainty values for the flux and velocity are shown as error bars in the right side of each panel.

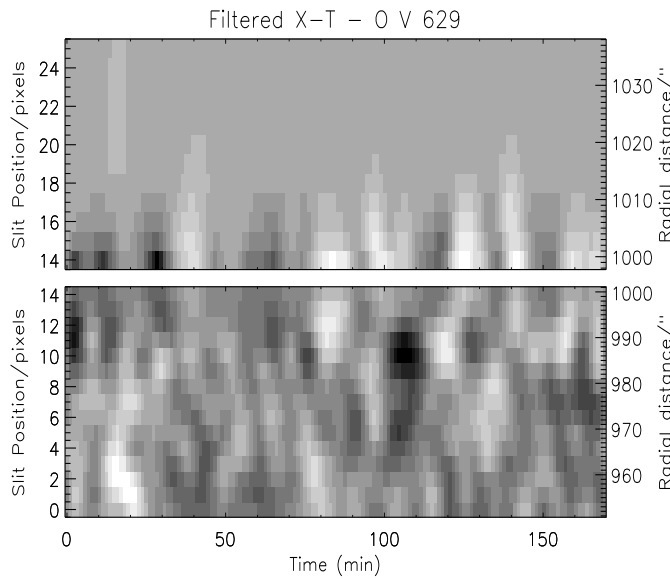


**Fig. 4.** X-T plot for dataset 26438 showing the region between 14–25 pixels ( $\approx 1000$ – $1040''$ ), top panel, and the region between 0–14 pixels ( $\approx 950$ – $1000''$ ), bottom panel. The top panel image shows the square-root values of the flux, in order to enhance weaker features.

similar behaviour. It is known that spicule behaviour is characteristic of the transition region, although macro-spicule activity can reach higher altitudes, e.g. Pike & Mason (1998), Banerjee et al. (2000). In Fig. 5, we plot the equivalent X-T plot for the 26406 dataset. Here the evidence for macro-spicule activity is present out to above  $1030''$ . If we take one location in this X-T plot, pixel no. 18, equivalent to a height of  $\approx 1013''$ , and plot the flux and velocity for the four lines we get the result shown in Fig. 6. It is instantly clear from the upper panel that the O v is the only one to show significant flux variations, the coronal lines being weak off-limb. In addition, in the lower panel,

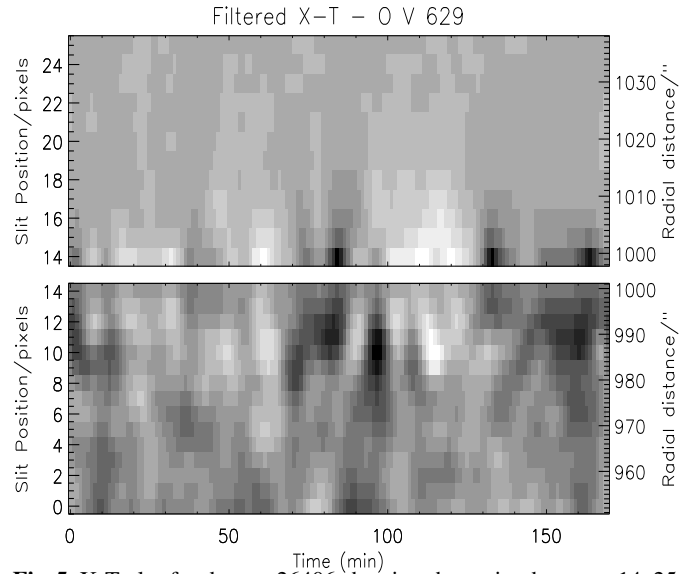


**Fig. 5.** X-T plot for dataset 26406 showing the region between 14–25 pixels ( $\approx 1000$ – $1040''$ ), top panel, and the region between 0–14 pixels ( $\approx 950$ – $1000''$ ), bottom panel. The top panel image shows the square-root values of the flux, in order to enhance weaker features.

the O v line is the only one to show significant velocities, the large uncertainties in the coronal lines of Mg x and Si xii making their measured velocities unreliable. It was noticed that the pattern of flux enhancement of the O v line in these off-limb locations bears a resemblance to those seen in blinker studies on the disk. In order to show that these can be defined as blinkers we plot in Fig. 7 the relative flux and the L.O.S. velocity for the O v line at the same location, pixel no.18, as shown in Fig. 6. The shaded areas in this figure show the parts of the enhanced flux that can be considered as a ‘blinker’, following the blinker identification method of Brković et al (2001) (see that paper for further details). The solid horizontal line in the plot shows the threshold value used in our identification, 1.45, while the dotted and dot-dash lines indicate the background and the background plus  $1\sigma$  standard deviation. Looking at this plot, we can see that there are three distinct groups of blinkers, the first between  $\approx 10$ – $40$  min, the second between  $\approx 40$ – $85$  min, and the third between  $\approx 85$ – $135$  min. These blinkers are anti-correlated with the L.O.S. velocity. This is readily apparent if one compares the L.O.S. velocities plotted as grey with the blinker flux plotted in black. For the first group of blinkers the correlation coefficient (calculated using the CORRELATE function in IDL) has a value of  $-0.64$ , for the second group a value of  $-0.50$  and for the third group a value of  $-0.85$ . This suggests a significant anti-correlation present in the first and third groups. This anti-correlation is not seen at all points along the slit. The locations outside of the blinker zone, which in this work can be defined as being between 14–25 pixels or  $\approx 1000''$ – $1040''$ , do not show this anti-correlation, e.g., see the plots in Fig. 3. This anti-correlation suggests that each brightening caused by the blinker event results in a significant blue-shift of material, while conversely darkenings result in a significant red-shift of material. These could be signatures of an up-flow of plasma in a spicule-like event, resulting in a brightening and a blue-shift,

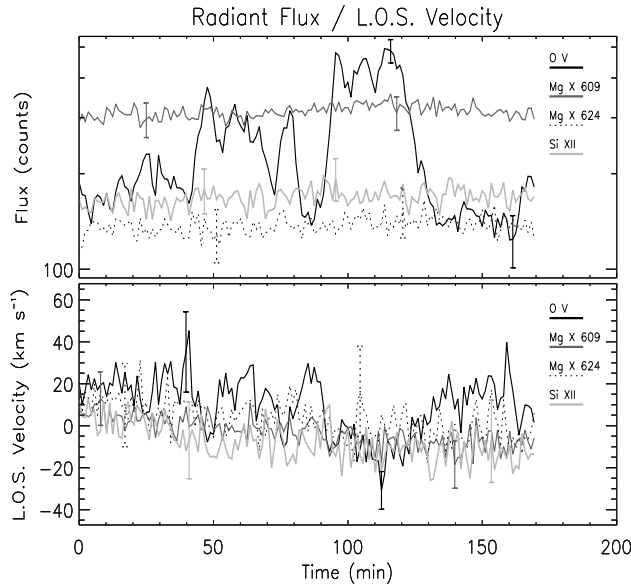


**Fig. 6.** Variation of flux with time (top panel) and variation of L.O.S. velocity with time (bottom panel) for pixel 18 of dataset 26406.

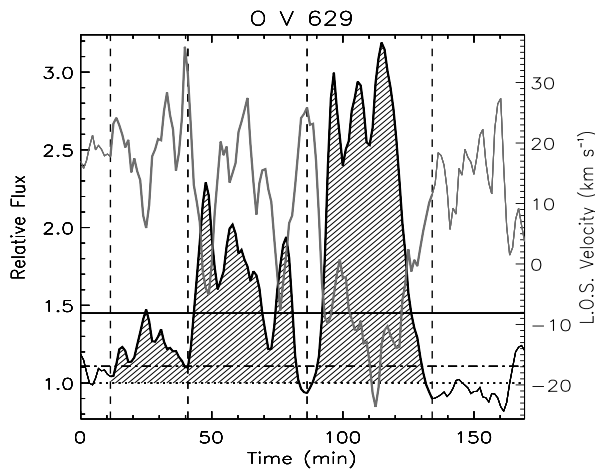


**Fig. 7.** Time series showing the relative flux and L.O.S. velocity (grey line) of the O v line at pixel position 18 of dataset 26406. Blinkers marked as dashed areas with different groups separated by the vertical dashed lines. The solid horizontal line in the plot shows the threshold value used in our identification, 1.45, while the dotted and dot-dash lines indicate the background and the background plus  $1\sigma$  standard deviation, respectively.

followed by a falling back of this plasma under gravity, resulting in a corresponding red-shift.

In Fig. 8 we show an example of a blinker found at pixel position 17 in dataset 26438. At this location it can be seen from the plot that there are four blinker groups with anti-correlation coefficients of  $-0.85$ ,  $-0.50$ ,  $-0.66$  and  $-0.85$  between  $\approx 30$ – $50$ ,  $90$ – $120$ ,  $120$ – $130$  and  $130$ – $150$  min, respectively.

#### 4. Conclusions

Following the ‘recipe’ for identifying blinkers, as outlined in Brković et al. (2001), we are able to say that blinkers are present at locations off-limb. We find these blinkers to be occurring above regions of dynamic activity, that produce evacuation events and quasi-periodic oscillations. We suggest that

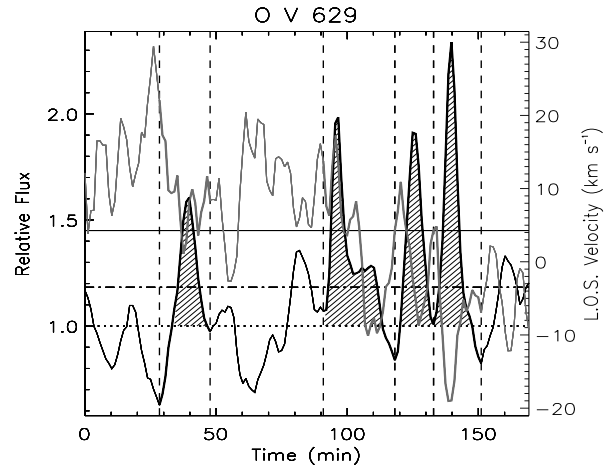


**Fig. 8.** Time series showing the relative flux and L.O.S. velocity (grey line) of the O v line at pixel position 17 of dataset 26438. Blinkers marked as dashed areas with different groups separated by the vertical dashed lines.

the blinkers seen are signatures of macro-spicules present at the temperature of the O v line. These results would suggest that blinkers, including those on the disk, are likely the result of heating of cool spicular material (Priest et al. 2002).

*Acknowledgements.* We would like to thank the CDS team at RAL and at Goddard Space Flight Center for their help in obtaining and reducing the data. CDS is part of SOHO, the Solar and Heliospheric Observatory, which is a project of international cooperation between ESA and NASA. This work was supported in part by a PRTL research grant for Grid-enabled Computational Physics of Natural Phenomena (Cosmogrid). We thank the referee, A. Brković, for his careful reading of the paper.

#### References

- Banerjee, D., O’Shea, E. & Doyle, J.G., 2000, *A&A* 355, 1152
- Bewsher, D., Innes, D.E., Parnell, C.E., Brown, D.S., 2005, *A&A*, 432, 307
- Bewsher, D., Parnell, C.E., Harrison, R.A., 2002, *Sol. Phys.*, 206, 21
- Brković, A., Solanki, S.K., Rüedi, I., 2001, *A&A*, 373, 1056
- Brković, A., Peter, A., 2004, *A&A*, 422, 709
- Doyle, J.G., Giannikakis, J., Xia, L.D. & Madjarska, M.S., 2005, *A&A*, 431, L17
- Harrison, R.A., Sawyer, E.C., Carter, M.K., Cruise, A.M., et al., 1995, *Sol. Phys.*, 162, 233
- Harrison R.A., 1997, *Sol. Phys.*, 392, 319
- Harrison R.A., Lang, J., Brooks, D.H., Innes, D.E., 1999, *A&A*, 351, 1115
- Madjarska, M.S., Doyle, J.G., 2003, *A&A*, 403, 731
- O’Shea, E., Banerjee, D., Doyle, J.G., 2005, *A&A* (in press)
- Pike, C.D. & Mason, H.E., 1998, *Sol Phys* 182, 333
- Priest, E.R., Wood, A.W., Bewsher, D., 2002, *Sol. Phys.*, 205, 249
- Wilhelm, K., 2000, *A&A*, 360, 351
- Xia, L.D., Popescu, M.D., Doyle, J.G. & Giannikakis, J., 2005, *A&A* (in press)